Optik 151 (2017) 98–109

Contents lists available at ScienceDirect

Optik

journal homepage: www.elsevier.de/ijleo

Original research article

BER analysis and power control for interfering visible light communication systems☆

Yi Chen[a,b,*], Chi Wan Sung[c], Siu-Wai Ho[d], Wing Shing Wong[e]

[a] School of Science and Engineering, The Chinese University of Hong Kong, Shenzhen, China
[b] Shenzhen Research Institute of Big Data, Shenzhen, China
[c] Department of Electronic Engineering, City University of Hong Kong, Hong Kong
[d] Institute for Telecommunication Research, University of South Australia, Australia
[e] Department of Information Engineering, The Chinese University of Hong Kong, China

ARTICLE INFO

Article history:
Received 20 March 2017
Received in revised form 22 July 2017
Accepted 23 October 2017

Keywords:
Visible light communication
Interference model
Bit error rate
Power control

ABSTRACT

This paper studies the error performance of visible light communication systems consisting of multiple transmitter–receiver pairs, where mutual interference exists. Unlike the traditional method which approximates the interference signal as a Gaussian random process and express the bit error rate (BER) as a function of the signal-to-interference-plus-noise power ratio (SINR), we conduct a detailed analysis that captures the signal structure of the interference in terms of the number of light sources, and derive the BER explicitly. Simulation results show that under a realistic small-room scenario with basic illumination requirement, the BER predicted by the Gaussian model is much higher than the exact BER. To provide an alternative metric for resource allocation purpose, we also propose a new approximate expression for the BER. A power control problem is further investigated to ensure that the system is operated in an effective manner.

1. Introduction

Visible light communication (VLC) is an emerging technology for indoor optical wireless communication. It makes use of light emitting diodes (LED) as transmitters, and provides illumination and data communication simultaneously [2]. Comparing with traditional radio frequency (RF) communications, VLC has many advantages such as, it can use unregulated and license-free visible electromagnetic (EM) spectrum to transmit data and it does not interfere with existing RF systems. Besides, optical wireless signal provides higher security since it is very difficult for an eavesdropper to pick up the signal from outside the room. The first IEEE standard for VLC was published in 2011 in [3], which represents a significant milestone in promoting deployment of VLC.

In the past few years, many research activities have been done towards developing indoor high data rate VLC systems [4,5]. These efforts include the circuit design [6,7], channel modeling [8,9], modulation and coding schemes design [10,11], multiple-input-multiple-output (MIMO) techniques [12,13], etc. Among all these works, the most commonly used perfor-

☆ Part of the results has appeared in CSNDSP'16 [1]. This work is supported in part by an NSFC Grant No. 61701425. This work is supported in part by a grant from City University of Hong Kong under Project 7004238. This work is supported in part by a grant from the Research Grants Council of the Hong Kong Special Administrative Region, China under Project 414012.

* Corresponding author at: School of Science and Engineering, The Chinese University of Hong Kong, Shenzhen, China.
E-mail addresses: yichen@cuhk.edu.cn (Y. Chen), albert.sung@cityu.edu.hk (C.W. Sung), siuwai.ho@unisa.edu.au (S.-W. Ho), wswong@ie.cuhk.edu.hk (W.S. Wong).

https://doi.org/10.1016/j.ijleo.2017.10.124
0030-4026/

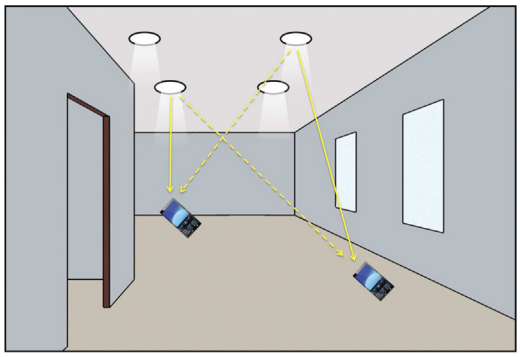

Fig. 1. An illustration of a VLC network consisting of two pairs of transmitter–receiver. The solid lines represent intended links and the dashed lines represent interfering links.
Reproduced from [15].

mance metric to measure the transmission quality of VLC is the signal-to-noise-ratio (SNR), which is defined as the power of the signal divided by the power of the noise. It is well known that under the condition of noise being additive white Gaussian, SNR can be mapped to BER directly. For example, the BER of non-return-to-zero (NRZ) on–off keying (OOK) is $Q(\sqrt{SNR}/2)$ and the BER of pulse amplitude modulation with M possible pulse amplitudes (M-PAM) is $Q(\sqrt{SNR\log_2 M}/(2M-2))$ [14]. However, if the noise is not Gaussian distributed, SNR may fail to have a clearly understood implication on BER. The error performance analysis of a VLC system under such case has seldom been considered.

In this paper, we consider an indoor VLC network consisting of multiple transmitter–receiver pairs, as illustrated in Fig. 1. Such scenario is analogous to today's cellular network where each LED is a base station and serves the users within its coverage area. Due to the broadcast nature of wireless channels, interference arises whenever multiple transmitter–receiver pairs are active concurrently in the same frequency band, and each receiver is only interested in retrieving information from its own transmitter. For a particular receiver, the received signal is a superposition of its desired signal, interfering signals and noise. Most of existing papers (e.g., [16–18] and the references therein) treat interference as another source of noise and define SINR as the performance metric, similar to SNR. Using SINR as a surrogate for BER implicitly assumes that the interference is a Gaussian process. This Gaussian interference assumption can be partially justified by the central limit theorem (CLT) if the interference comes from mutually independent, identically distributed interferer signal processes and if the number of such interferers is large. If there are only a few interferers, the CLT is not applicable. For an indoor VLC network, the number of transmitter–receiver pairs is typically small due to the limited number of LEDs in a room area, and therefore the CLT may not be applicable. If the interference is far from Gaussian, the significance of SINR as a performance metric is less clear. References [19,20] have proposed a more accurate interference model for an RF system and showed that the Gaussian interference assumption did yield inaccurate BER, which could be overestimated or underestimated. In this paper, we dispense with the Gaussian assumption on the interference and analyze the BER for VLC systems using OOK, which is one of the most commonly used modulation schemes in VLC (see e.g., [6,10,21]). We derive the BER expressions under an exact analysis and under the Gaussian model, and perform simulations to compare them. It is shown in an example of four pairs of transmitter–receiver that the Gaussian interference model is generally pessimistic.

In the second part of this paper, to facilitate effective resource allocation for VLC systems, we propose a new approximation on BER and derive an upper bound on BER under certain technical conditions. The approximated BER and the BER upper bound are numerically shown to be close to the exact BER. Based on the BER bound, we then investigate a power control problem for an interfering VLC system, which is to minimize the total power of all LEDs, subject to some constraints of BER, illumination and power range requirements. It turns out that this optimization problem is a non-convex quadratically constrained linear programming. We propose an algorithm by means of successive convex approximation, which is guaranteed to converge to a feasible solution with good, if not optimal objective value. Simulations are carried out to see the performance of the proposed algorithm.

The rest of the paper is organized as follows. Section 2 gives the preliminary. The system model and BER analysis are presented in Sections 3 and 4, respectively. Section 5 provides simulation results under a realistic setting. In Section 6, a new method of approximation on BER is discussed. Section 7 investigates a power control problem. Some concluding remarks are offered in Section 8.

2. Preliminary

In an indoor VLC system, LEDs are used as transmitters and photodiodes are used as receivers. Assume that the LEDs are all in line-of-sight (LOS) of the receivers. In this section, we explain the channel gain and noise variance in VLC systems, which will be used later.

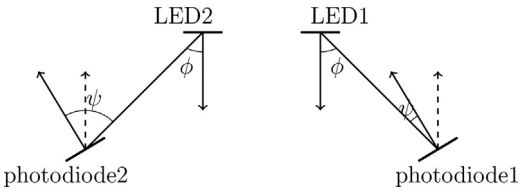

Fig. 2. Irradiance angle and incident angle.

Table 1
Parameters [8,22].

R_p	Photodetector responsivity	22 nA/lux (2.933×10^{-2} A/W)
q	Electronic charge	1.6×10^{-19} C
A_r	Effective area of photodiode	15 mm^2
B	Receiver bandwidth	100 MHz
I_{bg}	Background dark current	10 nA
I_2	Noise bandwidth factor	0.562
I_3		0.0868
k	Boltzmann constant	1.38×10^{-23} m^2 kg s^{-2} K^{-1}
T_k	Absolute temperature	295 K
G	Open-loop voltage gain	10
C	Capacitance	112×10^{-8} F/m^2 (s^4 A^2 m^{-4} kg^{-1})
Γ	FET channel noise factor	1.5
g_m	FET transconductance	0.03 S (kg^{-1} m^{-2} s^3 A^2)

A = Ampere, C = Coulomb, m = metre, s = second, K = Kelvin, W = Watt, kg = kilogram, F = Farad, S = Siemens.

2.1. Channel gain

For Lambertian radiation pattern of the transmitting LED, the LOS link gain can be derived as [2,8]

$$h = \frac{(m+1)A_r}{2\pi D^2}\cos^m(\phi)T(\psi)g(\psi)\cos(\psi), \tag{1}$$

where the parameters are defined as follows. A_r is the effective area of the receiver photodiode. D is the transmitter–receiver distance. ϕ is the irradiance angle with respect to the normal at the transmitter and ψ is the incident angle with respect to the normal at the receiver (see Fig. 2). $T(\psi)$ and $g(\psi)$ are the filter gain and concentrator gain at the receiver, respectively. In this paper, we assume $T(\psi) = g(\psi) = 1$. m is the Lambertian parameters given by $m = \frac{-\ln 2}{\ln(\cos(\phi_{1/2}))}$, where $\phi_{1/2}$ is the half-power angle of LED. Note that the receivers are not necessary to be horizontal. When a receiver is horizontal, $\psi = \phi$.

2.2. Noise

At the receiver, the photodiode current is affected by two noise processes: shot noise and thermal noise. The shot noise is related to the incident optical power and its variance (in A^2) is given by [2,8]

$$\sigma^2_{shot} = 2qR_pP_rB + 2qI_{bg}I_2B, \tag{2}$$

where P_r (in Watt) is the received optical power and the definitions of other parameters can be found in Table 1. The thermal noise variance (in A^2) is independent of the incident power and is given by [2,8]

$$\sigma^2_{thermal} = \frac{8\pi kT_k}{G}CA_rI_2B^2 + \frac{16\pi^2kT_k\Gamma}{g_m}C^2A_r^2I_3B^3, \tag{3}$$

where the parameters are defined in Table 1. The total noise variance is

$$\sigma^2_{noise} = \sigma^2_{shot} + \sigma^2_{thermal}. \tag{4}$$

In Ref. [22], measurement results show that none of the shot noise and thermal noise can be ignored. We can also get this conclusion by the following calculation. The typical values of the parameters in (3) are listed in Table 1. By substituting them into (3), we have $\sigma^2_{thermal} = 17.5348 \times 10^{-16}$ A^2. In practice, the standard illumination level for most indoor environments (classroom, conference-room, lecture hall, offices, etc.) is between 300 and 500 lux at 0.8 m height from the floor. This is equivalent to a power requirement of $p_r \geq 2.25 \times 10^{-4}$ W (assuming $\psi = \phi$). Therefore according to (2) the shot noise variance should be at least 2.1120×10^{-16} A^2 and is on the same level as that of thermal noise. In the subsequent analysis of BER, we will incorporate both the shot noise and thermal noise, where the model is different from that in RF systems without shot noise issue (e.g., [19]).

3. System model

Consider a room where there are N LED transmitters being installed on the ceiling and they are denoted by $\{LED_i : i = 1, \ldots, N\}$. Besides the function of lighting, these N LEDs are used to transmit different data to N receivers $\{rec_i : i = 1, \ldots, N\}$, which could be mobile devices equipped with photodiodes. In particular, LED_i intends to transmit data to rec_i and there are N transmitter–receiver pairs. Fig. 1 illustrates an example of a two-pair system. Assume that the LEDs transmit data separately without any central unit controlling, and no cooperation between them is allowed. All transmissions use the same wavelength carrier and thus cause interference to each other.

In this paper, the OOK modulation scheme with NRZ code is considered. It is possible to use the mathematical technique in this paper to analyze other modulation schemes like PAM but this is reserved for future work. The information bits of LED_i are denoted by $\{b_i^k\}_{k=-\infty}^{\infty}$ where b_i^k is uniformly distributed on $\{0, 1\}$. The LED is on when $b_i^k = 1$ and is off when $b_i^k = 0$. Let rect(t) be the unit-amplitude rectangular pulse of duration T, where $T = 1/B$. The transmitted optical signal $s_i(t)$ of LED_i is

$$s_i(t) = p_i \sum_{k=-\infty}^{\infty} b_i^k rect(t - kT), \tag{5}$$

where p_i (in Watt) is the peak optical power of the light wave emitter. The average transmitted power is $p_i/2$. Denote $\mathbf{p} = [p_1, \ldots, p_N]$ to be the power vector of the system.

Assume that the LEDs are all in LOS of the receivers. Let h_{ij} and d_{ij} denote the LOS optical channel gain and delay offset from LED_j to rec_i, respectively. The received electric signal at the photodiode of rec_i is

$$r_i(t) = \sum_{j=1}^{N} R_p h_{ij} s_j(t - d_{ij}) + n_i(t), \tag{6}$$

where R_p is the responsivity of the photodiode and $n_i(t)$ is the noise. As explained in the preliminary, the noise is a combination of shot noise and thermal noise. We model them as the additive white Gaussian noise (AWGN) with two-sided power spectral density N_{s_i} and N_t, respectively.

A receiver demodulates the received signal using a matched filter, followed by a threshold decision. The impulse response $s_i^0(t)$ of the filter of rec_i is a rectangular pulse of amplitude 1 and duration T. Assume $d_{ii} = 0$, that is, the matched filter of rec_i is synchronized to the arrival signal transmitted by LED_i. Consider a bit interval as $[0, T]$ to be demodulated. Label the first bit overlapping with this interval by b_j^0 for all $j = 1, \ldots, N$ and the following bit by b_j^1. We use $\tau_{ij} \in [0, 1)$ to denote the normalized (by T) misalignment of b_j^0 with respect to b_i^0. In calculating the average BER, we assume that the receivers are static over the averaging period so that τ_{ij}s are all constants.

After matched filtering, the input to the decision device for rec_i is given by

$$y_i = \frac{1}{T} \int_0^T r_i(t) s_i^0(t) \mathrm{d}t \tag{7}$$

$$= p_i h_{ii} b_i^0 R_p + \sum_{j \neq i} p_j h_{ij} [\tau_{ij} b_j^0 + (1 - \tau_{ij}) b_j^1] R_p + n_i \tag{8}$$

$$= p_i h_{ii} b_i^0 R_p + \sum_{j \neq i} p_j h_{ij} W_{ij} R_p + n_i, \tag{9}$$

where

$$W_{ij} = \tau_{ij} b_j^0 + (1 - \tau_{ij}) b_j^1 \quad for \quad j \neq i \tag{10}$$

is a discrete random variable uniformly distributed over $\{\tau_{ij}, 1 - \tau_{ij}, 1, 0\}$, and

$$n_i = \frac{1}{T} \int_0^T n_i(t) s_i^0(t) \mathrm{d}t \tag{11}$$

is a Gaussian random variable with zero mean and variance $(N_{s_i} B + N_t B)$. The variance of the thermal noise $N_t B$ is decided by (3) and is independent of the incident power. The variance of the shot noise is decided by (2) as

$$N_{s_i} B = 2q(p_i h_{ii} b_i^0 R_p + \sum_{j \neq i} p_j h_{ij} W_{ij} R_p) B + 2q I_{bg} I_2 B, \tag{12}$$

and is dependent on the incident power. For notation simplicity, we use $\sigma_c^2 = 2q I_{bg} I_2 B + N_t B$ to denote the constant part of the variance of the total noise.

4. Analysis of bit error rate

In this section, we first present an exact analysis of BER. Then, we present an approximate analysis, which makes a simplifying assumption that the interference term is Gaussian distributed.

4.1. Exact analysis

Let ξ_i be the decision threshold of rec_i. An error occurs if $y_i > \xi_i$ when $b_i = 0$ or if $y_i < \xi_i$ when $b_i = 1$. Conditioned on W_{ij} for all $j \neq i$, the error rates are

$$p_r\{y_i > \xi_i | b_i^0 = 0, W_{ij}, j \neq i\} = Q\left(\frac{\xi_i - \sum_{j\neq i} p_j h_{ij} W_{ij} R_p}{\sqrt{2}}\right), \tag{13}$$

$$p_r\{y_i < \xi_i | b_i^0 = 1, W_{ij}, j \neq i\} = Q\left(\frac{p_i h_{ii} R_p + \sum_{j\neq i} p_j h_{ij} W_{ij} R_p - \xi_i}{\sqrt{2}}\right). \tag{14}$$

The average BER of the ith transmitter–receiver pair is

$$P_{e_i} = \frac{1}{4^{N-1}} \sum_{W_{iN}\in\{\tau_{iN}, 1-\tau_{iN}, 1, 0\}} \cdots \sum_{W_{i1}\in\{\tau_{i1}, 1-\tau_{i1}, 1, 0\}} \left[\frac{1}{2} Q\left(\frac{\xi_i - \sum_{j\neq i} p_j h_{ij} W_{ij} R_p}{\sqrt{2q\sum_{j\neq i} p_j h_{ij} W_{ij} R_p B + \sigma_c^2}}\right) + \frac{1}{2} Q\left(\frac{p_i h_{ii} R_p + \sum_{j\neq i} p_j h_{ij} W_{ij} R_p - \xi_i}{\sqrt{2q(p_i h_{ii} R_p + \sum_{j\neq i} p_j h_{ij} W_{ij} R_p)B + \sigma_c^2}}\right)\right]. \tag{15}$$

4.2. Gaussian approximation

In the literature, it is common to treat interference as white Gaussian noise. That is, the interference term $\sum_{j\neq i} p_j h_{ij} W_{ij} R_p$ in (9) is approximated by a Gaussian random variable with identical mean and variance. We simply call this model as *Gaussian interference model*.

For the Gaussian interference model, the mean and variance of the interference term $\sum_{j\neq i} p_j h_{ij} W_{ij} R_p$ can be calculated by averaging over W_{ij} for all $j \neq i$. As mentioned before, W_{ij} takes values from $\{\tau_{ij}, 1-\tau_{ij}, 1, 0\}$ with equal probability. We get that the mean is $\frac{1}{2}\sum_{j\neq i} p_j h_{ij} R_p$ and the variance is $\sigma_I^2 = \sum_{j\neq i} p_j^2 h_{ij}^2 R_p^2 (\frac{1}{2}\tau_{ij}^2 - \frac{1}{2}\tau_{ij} + \frac{1}{4})$. The shot noise variance under the Gaussian interference model becomes

$$N_{s_i} B = 2qp_i h_{ii} b_i^0 R_p B + 2qI_{bg} I_2 B. \tag{16}$$

Hence the BER can be derived as

$$P_{e_i}^G = \frac{1}{2} Q\left(\frac{\xi_i - (1/2)\sum_{j\neq i} p_j h_{ij} R_p}{\sqrt{\sigma_I^2 + \sigma_c^2}}\right) + (1/2) Q\left(\frac{p_i h_{ii} R_p + (1/2)\sum_{j\neq i} p_j h_{ij} R_p - \xi_i}{\sqrt{\sigma_I^2 + 2qp_i h_{ii} R_p B + \sigma_c^2}}\right). \tag{17}$$

The BER analysis in this section works for any number of transmitter–receiver pairs. In the next section, we carry out a simulation study to compare the BER performance under the Gaussian interference model with the exact BER.

5. Simulation studies

Consider a room of length 5 m, breadth 3 m and height 2.7 m. Four LEDs are installed on the ceiling as transmitters whose coordinates are LED_1(1.2, 0.5, 2.7), LED_2(3.8, 0.5, 2.7), LED_3(1.2, 2.5, 2.7) and LED_4(3.8, 2.5, 2.7), as illustrated in Fig. 3. Each LED is assumed to have a typical luminous flux of 6000 lumens (lm) and a luminous efficacy of 117 lm/W, which are the same as those of bridgelux LEDs (BXRA-56C5300-H-00) [23]. A receiver is put on the desk at a height of 0.83 m from the floor. It is equipped with a photodiode, which is used to measure the incident light intensity. The responsivity and effective area of this photodiode are given in Table 1. The configurations of the LEDs and photodiodes are the same as those used in [22]. The Lambertian parameter is $m = 1$. Given that the coordinates of a transmitter and a receiver are (x_t, y_t, z_t) and (x_r, y_r, z_r), the irradiance angle is given by

$$\phi = \arccos\left(\frac{|z_t - z_r|}{\sqrt{(x_t - x_r)^2 + (y_t - y_r)^2 + (z_t - z_r)^2}}\right). \tag{18}$$

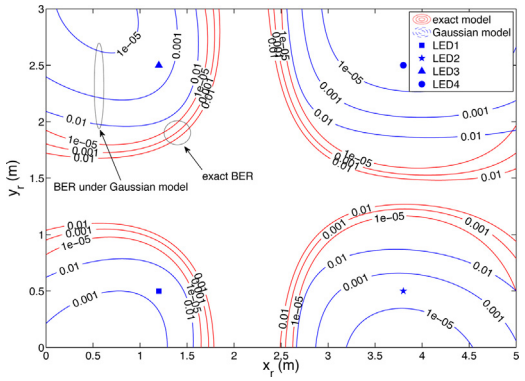

Fig. 3. The contour plot of BER for levels of 10^{-5}, 10^{-3}, 10^{-2} over the (x_r, y_r) plane under the exact analysis and the Gaussian interference model.

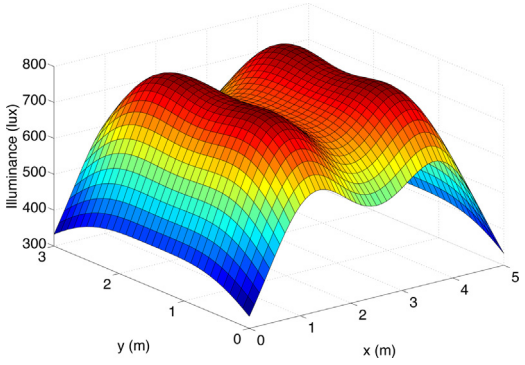

Fig. 4. The distribution of illuminance in a room.

The incident angle also depends on the orientation of the photodiode. If the photodiode's normal is parallel to the normal of the transmitter, then $\psi = \phi$. Otherwise assume that the normal of the photodiode is parallel to the vector $\mathbf{v}_n = [x_n, y_n, z_n]^T$. Let $\mathbf{v}_{rt} = [x_t - x_r, y_t - y_r, z_t - z_r]^T$. The incident angle can be calculated by

$$\psi = \arccos\left(\frac{\mathbf{v}_n^T \mathbf{v}_{rt}}{||\mathbf{v}_n|| \cdot ||\mathbf{v}_{rt}||}\right). \tag{19}$$

Let L be the luminous flux of an LED (in lumen) and D is the distance between transmitter and receiver. The illuminance (in lux) at a point (x_r, y_r, z_r) is given by [8]

$$I = L\frac{(m+1)\cos^m(\phi)\cos(\psi)}{2\pi D^2}. \tag{20}$$

Fig. 4 depicts the distribution of illuminance at a height of 0.83 m from the floor (assuming $\psi = \phi$) when the four LEDs are turned on and each has luminous flux of 6000 lm. It can be seen that this LED setting satisfies the typical lighting requirement of 300 lux, which shows that our parameter setting is realistic.

Next, we consider the BER performance for such an indoor VLC network. Consider that there is a receiver at the location $(x_r, y_r, 0.83)$ and the normal of its photodiode is $\mathbf{v}_n = [x_n, y_n, z_n]^T$. We can figure out the link gains between the receiver and the four LED transmitters by (1). Assume that the receiver's dedicated transmitter is the LED that has the largest link gain, and the remaining three LED transmitters are treated as interferers. For each position of the receiver, the exact BER and the BER under the Gaussian interference model can be calculated by (15) and (17), respectively. Fig. 3 gives the contour plot of BER for levels of 10^{-5}, 10^{-3} and 10^{-2} over the (x_r, y_r) plane of the room. In this example, all the transmitters are assumed to be synchronized (i.e., $\tau_{ij} = 0$ for all i, j) and use luminous flux of 6000 lm (i.e., 6000/117 = 51.2821 W). The normal of the receiver photodiode is set to be $\mathbf{v}_n = [\tan(30^\circ)\cos(20^\circ), \tan(30^\circ)\sin(20^\circ), 1]^T$, and is fixed for all the locations of the receiver. The decision threshold ξ is chosen as the one that minimizes the BER at each particular location, which is numerically obtained by one-dimensional search.

For Fig. 3, first it can be seen that the contour plot is asymmetric. This is due to the fact that the normal of the photodiode is not vertical. Second, the three curves representing different levels of BER under the Gaussian interference model are more separative than those under the exact model. Third, given the same location, that is, the same link gains setting, the BER under the Gaussian interference model overestimates the BER by certain orders. For example, at the locations where the BER is 10^{-5}, the BER under the Gaussian interference model is beyond 10^{-2}.

From this example, we see that for a typical indoor VLC system, it is far from accurate to approximate the interference as a Gaussian process. Moreover, as can be seen from Fig. 3, without controlling the emitting power of the LEDs, the BER in part of the area is too high for data communications. Therefore, next we will investigate the power control problem for a VLC system, so as to ensure that the system is operated in an effective manner. But before that, we first provide an approximate expression of the BER, which will be used in the discussion of power control.

6. A new BER approximation

For power control purpose, the Gaussian interference model is commonly used, since it allows power control to be considered without concerning the details of the structure of the physical signals. This model, however, is not accurate in estimating BER for small values of N, as we have seen in the previous section. To determine the exact BER in (15), it is necessary to determine the optimal decision threshold, which can only be done by one-dimensional search. This makes the expression difficult to be used for power control. To circumvent the need of numerically searching for the optimal threshold, in this section, we provide an approximate expression of the BER for which the optimal threshold can be found.

In the following, we restrict our discussion to the cases of channel gains and powers such that

$$p_i h_{ii} R_p \geq \sum_{j \neq i} p_j h_{ij} R_p \quad \text{for} \quad i = 1, \ldots, N. \tag{21}$$

The intuition behind this condition is that the intended signal is larger than the aggregated interfering signals, so as to guarantee certain communication quality. To see that this restriction is reasonable, assume on the contrary that $p_i h_{ii} R_p < \sum_{j \neq i} p_j h_{ij} R_p$. Then, we have

$$P_{e_i} \geq \frac{1}{4^{(N-1)}} \frac{1}{2} \left[Q\left(\frac{\xi_i - \sum_{j \neq i} p_j h_{ij} R_p}{\sqrt{2q \sum_{j \neq i} p_j h_{ij} R_p B + \sigma_c^2}} \right) + Q\left(\frac{p_i h_{ii} R_p - \xi_i}{\sqrt{2q p_i h_{ii} R_p B + \sigma_c^2}} \right) \right] \tag{22}$$

$$\geq \frac{1}{4^{(N-1)}} \frac{1}{2} Q(0) = \frac{1}{4^N}. \tag{23}$$

In (22), the first Q-item corresponds to the case when the intended bit is zero while all the interfering bits are one, i.e., $W_{ij} = 1$ for all $j \neq i$, and the second Q-item corresponds to the case when the intended bit is one while all the interfering bits are zero, i.e., $W_{ij} = 0$ for all $j \neq i$. The inequality holds because we have removed some non-negative terms from the exact BER expression in (15). The inequality in (23) holds since no matter what the threshold is chosen, at least one of $\xi_i - \sum_{j \neq i} p_j h_{ij} R_p$ and $p_i h_{ii} R_p - \xi_i$ is negative. In general, the maximum tolerable BER is considered to be 10^{-3} for voice and 10^{-7} for data. When $N = 4$, $P_{e_i} \geq 0.0039$, which is too high for data communications.

Ref. [19] gives the condition on the link gains when there exists a power vector $\mathbf{p} > \mathbf{0}$ such that $p_i h_{ii} \geq \sum_{j \neq i} p_j h_{ij}$ for all i. We state the results here for the completeness.

Theorem 1. [19]

For a system consisting of N pairs of transmitter–receiver, there exists a power allocation $\mathbf{p} > \mathbf{0}$ *such that* $p_i h_{ii} \geq \sum_{j \neq i} p_j h_{ij}$ *for* $i = 1, \ldots, N$, *if and only if the character matrix* $\mathbf{C} = (C_{ij})$, *defined as* $C_{ij} = -h_{ij}$ *for* $i \neq j$ *and* $C_{ii} = h_{ii}$ *for* $i, j = 1, \ldots, N$, *is an M-matrix, i.e., the eigenvalues of* $\mathbf{C}$ *all have positive real parts.*

If the link gains fail to satisfy the condition, scheduling is required to select candidate subsets of concurrently active transmitter–receiver pairs (that use the same wavelength carrier) and this is out of the scope of this paper. We also impose the condition that the decision threshold must satisfy $\sum_{j \neq i} p_j h_{ij} R_p \leq \xi_i \leq p_i h_{ii} R_p$ for all $i = 1, \ldots, N$. For the cases when the optimal threshold falls outside this range, the BER is greater than $\frac{1}{4^N}$ and is out of our interest. Under this condition, every Q-item in (15) has nonnegative entry. We note in (15) that the denominators in all Q-items are bounded above by $\sigma_i^2 = 2qB \sum_{j=1}^{N} p_j h_{ij} R_p + \sigma_c^2$. We replace all the denominators with σ_i^2 and approximate the BER by

$$\tilde{P}_{e_i} = \frac{1}{4^{N-1}} \sum_{W_{iN} \in \{\tau_{iN}, 1-\tau_{iN}, 0\}} \cdots \sum_{W_{i1} \in \{\tau_{i1}, 1-\tau_{i1}, 1, 0\}} \left[\frac{1}{2} Q\left(\frac{\xi_i - \sum_{j \neq i} p_j h_{ij} W_{ij} R_p}{\sigma_i} \right) + \frac{1}{2} Q\left(\frac{p_i h_{ii} R_p + \sum_{j \neq i} p_j h_{ij} W_{ij} R_p - \xi_i}{\sigma_i} \right) \right]. \tag{24}$$

Since the function $Q(x)$ is monotonically decreasing as x is increasing for $x \geq 0$, we always have $P_{e_i} \leq \tilde{P}_{e_i}$. For $\tilde{P}_{e_i}$, the optimal threshold can be found and is given by the following theorem, whose proof is provided in Appendix A.

Theorem 2. *For any* $i = 1, \ldots, N$, *if* $p_i h_{ii} R_p \geq \sum_{j \neq i} p_j h_{ij} R_p$, *the optimal threshold that minimizes* $\tilde{P}_{e_i}$ *and satisfies* $\sum_{j \neq i} p_j h_{ij} R_p \leq \xi_i \leq p_i h_{ii} R_p$ *is*

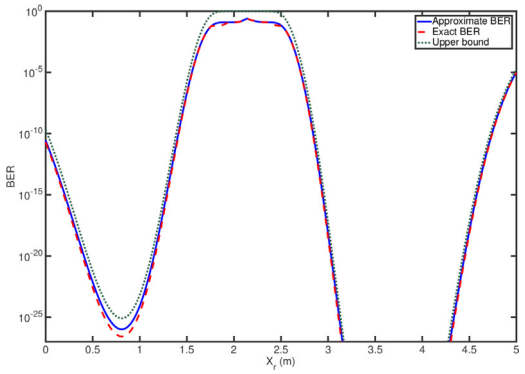

Fig. 5. The exact BER and the approximate BER. The receiver's location is $(x_r, 0.5, 0.83)$, i.e., on the straight line from LED_1 to LED_2.

$$\tilde{\xi}_i = \frac{1}{2}(p_i h_{ii} R_p + \sum_{j \neq i} p_j h_{ij} R_p). \tag{25}$$

At $\tilde{\xi}_i$, the bit error rate when $b_i^0 = 0$ is the same as the bit error rate when $b_i^0 = 1$. So $\tilde{P}_{e_i}$ becomes

$$\tilde{P}_{e_i} = \frac{1}{4^{N-1}} \sum_{W_{iN} \in \{\tau_{iN}, 1-\tau_{iN}, 1, 0\}} \cdots \sum_{W_{i1} \in \{\tau_{i1}, 1-\tau_{i1}, 1, 0\}} Q\left(\frac{(1/2)p_i h_{ii} R_p + \sum_{j \neq i} p_j h_{ij}((1/2) - W_{ij}) R_p}{\sigma_i}\right) \tag{26}$$

An upper bound of $\tilde{P}_{e_i}$ can be easily derived as

$$\tilde{P}_{e_i} \leq \tilde{P}_{e_i}^{bound} = Q\left(\frac{(1/2)p_i h_{ii} R_p - (1/2)\sum_{j \neq i} p_j h_{ij} R_p}{\sigma_i}\right), \tag{27}$$

since for every possible combination of $W_{ij}, j \neq i$, we always have

$$Q\left(\frac{(1/2)p_i h_{ii} R_p + \sum_{j \neq i} p_j h_{ij}((1/2) - W_{ij}) R_p}{\sigma_i}\right) \leq \tilde{P}_{e_i}^{bound}. \tag{28}$$

Since $P_{e_i} \leq \tilde{P}_{e_i}$, $\tilde{P}_{e_i}^{bound}$ is also an upper bound of the exact BER P_{e_i}.

Using the same example in Section 5 and fixing $y_r = 0.5$, Fig. 5 shows the exact BER P_{e_i} and the approximate BER $\tilde{P}_{e_i}$ versus x_r. The exact BER is obtained by numerically searching for the optimal value of ξ that minimizes (15). We see that the curve of approximate BER is always above the curve of exact BER, as expected. Besides, the two curves are close, and nearly overlap with each other at BER values of concern in the range of 10^{-10} through 10^{-3}. The intuition is that in VLC systems, the noise level is relatively small when compared with the signal level (see in (2), the thermal noise power is the signal power times qB where $q = 1.610^{-19}$ is small). So the BER mainly depends on the sign of $p_i h_{ii} R_p - \sum_{j \neq i} p_j h_{ij} R_p$ and when $p_i h_{ii} R_p \geq \sum_{j \neq i} p_j h_{ij} R_p$, our approximation by enlarging the noise power does not affect the result too much. This intuition also explains why the changes of BER are sharp around $x_r = 1.7$ and $x_r = 2.5$, where the condition (21) fails to be satisfied. The upper bound $\tilde{P}_{e_i}^{bound}$ is also plotted in Fig. 5, which shows that the bound is close to the exact BER as well. We also perform the same simulation for other values of y_r. Similar results are observed but omitted.

7. Power control

In this section, we consider a power control problem for VLC systems consisting of N transmitter–receiver pairs whose locations are fixed, and the channel gain between LED_j and rec_i is denoted by h_{ij} (ref. Section 3). Fig. 6 illustrates an example of four-pair system. The objective is to minimize the total transmitting power while guaranteeing that the BER requirement of each communication pair and the illumination requirement are satisfied. For the simplicity of analysis, the BER requirement considered here is that the upper bound of the average BER, i.e., $\tilde{P}_{e_i}^{bound}$, is below a threshold.

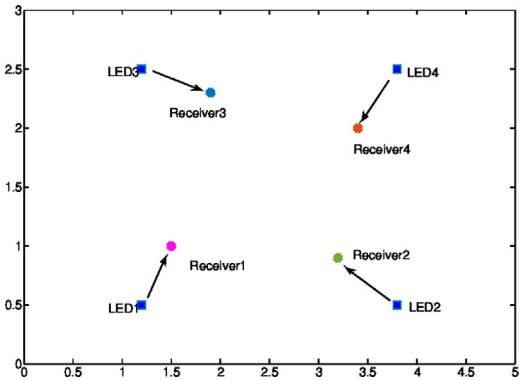

Fig. 6. In this VLC system, LED i communicates to Receiver i. The locations of Receiver 1 to 4 are (1.5, 1, 0.83), (3.2, 0.9, 0.83), (1.9, 2.3, 0.83) and (3.4, 2, 0.83).

Table 2
The resulting BER bound, approximate BER and exact BER with and without power control.

	p_i (W)	$\tilde{P}_{e_i}^{bound}$	$\tilde{P}_{e_i}$	P_{e_i}
With power control				
$i=1$	50.5217	10^{-5}	1.25×10^{-6}	0.9710×10^{-6}
$i=2$	55.4991	10^{-5}	1.25×10^{-6}	0.9693×10^{-6}
$i=3$	53.2476	10^{-5}	1.25×10^{-6}	0.9814×10^{-6}
$i=4$	53.6233	10^{-5}	1.25×10^{-6}	0.9636×10^{-6}
Without power control				
$i=1$	53.8462	1.4269×10^{-8}	1.7836×10^{-9}	1.1519×10^{-9}
$i=2$	53.8462	49.248×10^{-5}	61.560×10^{-6}	52.725×10^{-6}
$i=3$	53.8462	1.4965×10^{-5}	1.8706×10^{-6}	1.4789×10^{-6}
$i=4$	53.8462	0.5351×10^{-5}	0.6688×10^{-6}	0.5077×10^{-6}

As has been argued in the previous section, we assume that the channel gains satisfy that the character matrix (defined in Theorem 1) given below

$$\mathbf{C}=\begin{bmatrix} h_{11} & -h_{12} & \cdots & -h_{1N} \\ -h_{21} & h_{22} & \cdots & -h_{2N} \\ \vdots & \vdots & \ddots & \vdots \\ -h_{N1} & -h_{N2} & \cdots & h_{NN} \end{bmatrix} \tag{29}$$

is an M-matrix. Otherwise, the resulting BER can never be acceptable. Let $h_i(x, y)$ denote the channel gain from LED_i to a point located at $(x, y, 0.8)$, which is determined by (1). The power control problem is formulated as

$$\begin{aligned} \min \quad & \sum_{i=1}^{N} p_i \\ s.t. \quad & Q\left(\frac{(1/2)p_i h_{ii} R_p - (1/2)\sum_{j\neq i} p_j h_{ij} R_p}{\sqrt{2qB\sum_{j=1}^{N} p_j h_{ij} R_p + 2qI_{bg}I_2 B + N_t B}}\right) \leq \epsilon, \ \ i=1,\ldots,N, \\ & \sum_{i=1}^{N} \frac{h_i(x,y)}{A_r \alpha} p_i \geq \ell \ \ \forall x \in [0, \text{roomlength}], y \in [0, \text{roombreadth}], \\ & p_{\min} \leq p_i \leq p_{\max}, \ \ i=1,\ldots,N, \end{aligned} \tag{OP1}$$

where ϵ is the BER requirement threshold, ℓ is the illuminance requirement, α is the convert rate between power and luminous flux, A_r is the effective area of the receiver photodiode, p_{min} and p_{max} are the minimum and maximum allowable LED transmitting power. The first constraint guarantees that $\tilde{P}_{e_i}^{bound}$ (and thus the exact BER) is below a threshold for every transmission pair. The second constraint guarantees that the lighting requirement is satisfied at everywhere in the room. The

third constraint is imposed by the power condition of the LEDs. For notation simplicity, let $\gamma = (Q^{-1}(\epsilon)\cdot 2/R_p)^2$, $a = 2qBR_p$ and $b = 2qI_{bg}I_2B + N_tB$, which are all constants. Suppose $\epsilon \ll 0.5$, the first constraint can be rewritten as

$$p_i h_{ii} - \sum_{j\neq i} p_j h_{ij} \geq 0, \text{ and } \left(p_i h_{ii} - \sum_{j\neq i} p_j h_{ij}\right)^2 \geq \gamma \left(a\sum_{j=1}^{N} p_j h_{ij} + b\right), \quad i = 1, \ldots, N. \tag{30}$$

For $i = 1, \ldots, N$, define

$$\bar{\mathbf{h}}_\mathbf{i} = \begin{bmatrix} -h_{i1} \\ \vdots \\ -h_{ii-1} \\ h_{ii} \\ -h_{ii+1} \\ \vdots \\ -h_{iN} \end{bmatrix} \qquad \mathbf{h}_i = \begin{bmatrix} h_{i1} \\ \vdots \\ h_{ii-1} \\ h_{ii} \\ h_{ii+1} \\ \vdots \\ h_{iN} \end{bmatrix}.$$

Inequality contraint (30) is equivalent to $\bar{\mathrm{h}}_\mathrm{i}\mathbf{p} \geq 0$ and $\mathbf{p}^T\mathbf{H}_i\mathbf{p} \geq \mathbf{h}_i^T\mathbf{p}\cdot\gamma a + \gamma b$, where $\mathbf{H}_i = \bar{\mathrm{h}}_\mathrm{i}\bar{\mathrm{h}}_\mathrm{i}^{\,T}$ is a positive semidefinite matrix. For the illuminance requirement, instead of considering everywhere in the room, we uniformly sample M locations (e.g., the intersection points of the grids) to impose a finite number of constraints. Let (x_k, y_k) denote the kth location and let $\mathbf{c}_k = [\frac{h_1(x_k,y_k)}{A_r\alpha}, \ldots, \frac{h_N(x_k,y_k)}{A_r\alpha}]^T$ for $k = 1, \ldots, M$. Denote $\mathbf{1} = [1,\ldots,1]^T$ be an all-one vector. The power control problem (OP1) becomes

$$\min \ \mathbf{1}^T\mathbf{p} \tag{OP2}$$

$$\begin{aligned} s.t. \quad & -\mathbf{p}^T\mathbf{H}_i\mathbf{p} + \mathbf{h}_i^T\mathbf{p}\cdot\gamma a + \gamma b \leq 0, \quad i = 1, \ldots, N \quad \bar{\mathrm{h}}_\mathrm{i}\mathbf{p} \geq 0, \quad i = 1, \ldots, N \\ & \mathbf{c}_k\mathbf{p} \geq \ell, \quad k = 1, \ldots, M \\ & p_{\min} \leq p_i \leq p_{\max}, \quad i = 1, \ldots, N \end{aligned} \tag{31}$$

which is a quadratically constrained linear programming. Since the constraints (31) are non-convex, the optimization problem is non-convex. In the following, we propose an algorithm by means of successive convex approximation to find a solution. The rough idea is that at each iteration, we form a linear approximation of (31) by using its first order Taylor expansion, solve the approximate convex optimization problem, and use the resulting solution as input for next round. To be specific, let

$$f_i(\mathbf{p}) = -\mathbf{p}^T\mathbf{H}_i\mathbf{p} + \mathbf{h}_i^T\mathbf{p}\cdot\gamma a + \gamma b. \tag{32}$$

The first order Taylor expansion of $f_i(\mathbf{p})$ at $\mathbf{p}^{(r)}$ is

$$\tilde{f}_i\left(\mathbf{p}, \mathbf{p}^{(r)}\right) \triangleq f\left(\mathbf{p}^{(r)}\right) + \left(-2\mathbf{H}_i\mathbf{p}^{(r)} + \mathbf{h}_i\gamma a\right)^T\left(\mathbf{p} - \mathbf{p}^{(r)}\right), \tag{33}$$

which is a linear approximation. The algorithm is described in Algorithm 1. The proposed algorithm satisfies each of the conditions in [24] for the convergence of succesive convex approximation algorithms. The algorithm stops at a Karush–Kuhn–Tucker (KKT) point, and can find a feasible solution with good, if not optimal, objective value.

Algorithm 1. Successive convex approximation algorithm for solving (OP2)

$$\begin{aligned} \min \quad & \mathbf{1}^T\mathbf{p} \\ s.t. \quad & \tilde{f}_i(\mathbf{p}, \mathbf{p}^{(r)}) \leq 0, \quad i = \mathbf{1}, \ldots, N \\ & \bar{\mathrm{h}}_\mathrm{i}\mathbf{p} \geq 0, \quad i = \mathbf{1}, \ldots, N \\ & \mathbf{c}_k\mathbf{p} \geq \ell, \quad k = \mathbf{1}, \ldots, M \\ & p_{\min} \leq p_i \leq p_{\max}, \quad i = \mathbf{1}, \ldots, N \end{aligned}$$

Find a feasible point $\mathbf{p}^{(0)}$ in (OP2), and set $r=0$.
repeat
Set $\tilde{\mathbf{p}}^*$ be the optimal solution of the following optimization problem

$$\begin{aligned} \min \quad & \mathbf{1}^T\mathbf{p} \\ s.t. \quad & \tilde{f}_i(\mathbf{p}, \mathbf{p}^{(r)}) \le 0, \quad i = \mathbf{1}, \ldots, N \\ & \tilde{\mathrm{h}}_i\mathbf{p} \ge 0, \quad i = \mathbf{1}, \ldots, N \\ & \mathbf{c}_k\mathbf{p} \ge \ell, \quad k = \mathbf{1}, \ldots, M \\ & p_{\min} \le p_i \le p_{\max}, \quad i = \mathbf{1}, \ldots, N \end{aligned}$$

Set $r \longleftarrow r+1$
Set $\mathbf{p}^{(k)} = \tilde{\mathbf{p}}^*$
until some convergence criterion is met.

Next, we apply this algorithm to an example. Consider the setting given in Section 5. Now the four LEDs want to communicate with their corresponding receivers, respectively, as illustrated in Fig. 6. The four receivers are placed horizontal, i.e., their normals are vertical. Suppose that the bit error probability requirement is $\epsilon = 10^{-5}$, the illumination requirement is ℓ=300 lux, $p_{max} = 7500/117 = 64.1026$ W and $p_{min} = 5500/117 = 47.0085$ W. The convert rate between power and luminous flux is $\alpha = 1/117$ W/lm. We apply Algorithm 1 to find a power allocation which is a feasible solution to (OP2). In this example, it only takes three iterations for the algorithm to find the solution. The resulting BER bound $\tilde{P}_{e_i}^{bound}$, approximate BER $\tilde{P}_{e_i}$ and exact BER P_{e_i} of the four communication pairs are summarized in Table 2. The power solution guarantees that $\tilde{P}_{e_i}^{bound}$ satisfies the requirement 10^{-5} and the exact BER is below 10^{-6}. If power control is not performed, and each LED transmits with typical power $p_1 = p_2 = p_3 = p_4 = 6300/117 = 53.8462$ W, the resulting BERs are also given in Table 2. Without power control, the second and the third communication pairs fail to satisfy the requirement on $\tilde{P}_{e_i}^{bound}$ and have higher exact BER than the other two pairs. We point out that here the sum of power is $53.8462 \times 4 = 215.3848$, larger than that found by power control (which is 212.8917). If we choose smaller power than 53.8462 W for the four LEDs, the resulting BERs are worser and thus not reported here.

8. Concluding remarks

In this paper, we derived the exact BER expression for VLC systems where there are multiple transmitter–receiver pairs and interference exists. Unlike the traditional Gaussian interference model which only uses the first and the second moments of the interference, the signal structure of the interference and all of its statistics are preserved in our analysis. Simulation results showed that the BER predicted by the Gaussian interference model is not accurate in a small-room setting with four LEDs. Whether the Gaussian interference model is applicable in a large room with many LEDs requires further investigation.

In a VLC system, resource allocation such as power control is important to ensure that the system is operated in an effective manner. To perform power control, an accurate performance metric is important. While the exact BER can be analytically derived, calculating the BER requires numerically determining the optimal decision threshold of the matched filter output. To circumvent this difficulty, we proposed a new approximation for the BER, which is shown to be accurate by simulations. Finally, we used this metric to formulate a power control problem, which turned out to be non-convex. We proposed an algorithm based on the successive convex approximation method, which can produce a good power solution.

Appendix A. Proof of Theorem 2

Proof. For any fixed $i = 1, \ldots, N$, consider $\tilde{P}_{e_i}$ to be a function of ξ_i. Take the first order derivative of (24) with respect to ξ_i and evaluate it at $\tilde{\xi}_i$. We have

$$\left.\frac{\mathrm{d}\tilde{P}_{e_i}}{\mathrm{d}\xi_i}\right|_{\xi_i=\tilde{\xi}_i} = \frac{1}{4^{N-1}} \sum_{W_{iN}\in\{\tau_{iN},1-\tau_{iN},1,0\}} \cdots \sum_{W_{i1}\in\{\tau_{i1},1-\tau_{i1},1,0\}} \tag{A.1}$$

$$\left[\frac{-1}{2\sqrt{2\pi}\sigma_i}\exp\left(-\frac{((1/2)p_ih_{ii}R_p+\sum_{j\neq i}p_jh_{ij}((1/2)-W_{ij})R_p)^2}{2\sigma_i^2}\right)\right. \tag{A.2}$$

$$\left.+\frac{1}{2\sqrt{2\pi}\sigma_i}\exp\left(-\frac{((1/2)p_ih_{ii}R_p+\sum_{j\neq i}p_jh_{ij}(W_{ij}-(1/2))R_p)^2}{2\sigma_i^2}\right)\right]. \tag{A.3}$$

We know that W_{ij} takes values of $\{\tau_{ij}, 1-\tau_{ij}, 1, 0\}$. So the possible values of $\frac{1}{2}-W_{ij}$ and $W_{ij}-\frac{1}{2}$ are the same. Therefore $\left.\frac{d\tilde{P}_{e_i}}{d\tilde{\xi}_i}\right|_{\xi_i=\tilde{\xi}_i}=0$. The second order derivative of (24) with respect to ξ_i is

$$\frac{d^2\widetilde{P}_{e_i}}{d\xi_i^2}=\frac{1}{4^{N-1}}\sum_{j\neq i}\sum_{W_{ij}}\left[\frac{1}{2\sqrt{2}\sigma_i}\ exp\left(-\frac{\left(\xi_i-\sum_{j\neq i}p_jh_{ij}W_{ij}R_p\right)^2}{2\sigma_i^2}\right)\frac{2\left(\xi_i-\sum_{j\neq i}p_jh_{ij}W_{ij}R_p\right)}{2\sigma_i^2}\right. \tag{A.4}$$

$$\left.+\frac{1}{2\sqrt{2}\sigma_i}exp\left(-\frac{\left(p_ih_{ii}R_p+\sum_{j\neq i}p_jh_{ij}W_{ij}R_p-\xi_i\right)^2}{2\sigma_i^2}\right)\frac{2\left(p_ih_{ii}R_p+\sum_{j\neq i}p_jh_{ij}W_{ij}R_p-\xi_i\right)}{2\sigma_i^2}\right]. \tag{A.5}$$

References

[1] Y. Chen, C.W. Sung, S.-W. Ho, W.S. Wong, BER analysis for interfering visible light communication systems, Proc. CSNDSP'16 (2016) 1–6.
[2] Z. Ghassemlooy, L.N. Alves, S. Zvanovec, M.-A. Khalighi, Visible Light Communications: Theory and Applications, CRC Press, 2017.
[3] IEEE standard for local and metropolitan area networks part 15.7, Short-range wireless optical communication using visible light, IEEE Standard 802.15.7 (2011).
[4] D. Karunatilaka, F. Zafar, V. Kalavally, R. Parthiban, LED based indoor visible light communications: state of the art, IEEE Commun. Surveys Tuts. 17 (2015) 1649–1678.
[5] P.H. Pathak, X. Feng, P. Hu, P. Mohapatra, Visible light communication, networking, and sensing: a survey, potential and challenges, IEEE Commun. Surveys Tuts. 17 (2015) 2047–2077.
[6] N. Fujimoto, H. Mochizuki, 477 Mbit/s visible light transmission based on OOK-NRZ modulation using a single commercially available visible LED and a practical LED driver with a pre-emphasis circuit, Proc. OFC/NFOEC'13 (2013) 1–3.
[7] H. Li, X. Chen, B. Huang, D. Tang, H. Chen, High bandwidth visible light communications based on a post-equalization circuit, IEEE Photon. Technol. Lett. 26 (2014) 119–122.
[8] T. Komine, M. Nakagawa, Fundamental analysis for visible-light communication system using LED lights, IEEE Trans. Consum. Electron. 50 (2004) 100–107.
[9] F. Miramirkhani, M. Uysal, Channel modeling and characterization for visible light communications, IEEE Photon. J. 7 (2015) 1–16.
[10] S. Rajagopal, R. Roberts, S.-K. Lim, IEEE 802.15.7 visible light communication: modulation schemes and dimming support, IEEE Commun. Mag. 50 (2012) 72–82.
[11] L. Wu, Z. Zhang, J. Dang, H. Liu, Adaptive modulation schemes for visible light communications, J. Lightw. Technol. 33 (2015) 117–125.
[12] T. Fath, H. Haas, Performance comparison of MIMO techniques for optical wireless communications in indoor environments, IEEE Trans. Commun. 61 (2013) 733–742.
[13] Y. Hong, T. Wu, L.K. Chen, On the performance of adaptive MIMO-OFDM indoor visible light communications, IEEE Photon. Technol. Lett. 28 (2016) 907–910.
[14] T.Y. Elganimi, Article: Performance comparison between OOK, PPM and PAM modulation schemes for free space optical (FSO) communication systems: analytical study, Int. J. Comput. Appl. 79 (2013) 22–27.
[15] W. Zhang, M.I.S. Chowdhury, M. Kavehrad, Asynchronous indoor positioning system based on visible light communications, Opt. Eng. 53 (2014).
[16] N.-T. Le, Y.M. Jang, Resource allocation for multichannel broadcasting visible light communication, Opt. Commun. 355 (2015) 451–461.
[17] F. Jin, X. Li, R. Zhang, C. Dong, L. Hanzo, Resource allocation under delay-guarantee constraints for visible-light communication, IEEE Access 4 (2016) 7301–7312.
[18] H. Liu, P. Xia, Y. Chen, L. Wu, Interference graph-based dynamic frequency reuse in optical attocell networks, Opt. Commun. 402 (2017) 527–534.
[19] Y. Chen, W.S. Wong, Power control for non-Gaussian interference, IEEE Trans. Wireless Commun. 10 (2011) 2660–2669.
[20] Y. Chen, S. Yang, W.S. Wong, Exact non-Gaussian interference model for fading channels, IEEE Trans. Wireless Commun. 12 (2013) 168–179.
[21] J.K. Kwon, Inverse source coding for dimming in visible light communications using NRZ-OOK on reliable links, IEEE Photon. Technol. Lett. 22 (2010) 1455–1457.
[22] M. Yasir, S.-W. Ho, B.N. Vellambi, Indoor positioning system using visible light and accelerometer, J. Lightw. Technol. 32 (2014) 3306–3316.
[23] Bridgelux, RS Array Series LED, 2011.
[24] B.R. Marks, G.P. Wright, A general inner approximation algorithm for nonconvex mathematical programs, Oper. Res. 26 (1978) 681–683.